Forest Ecology and Management 595 (2025) 123010

Contents lists available at ScienceDirect

Forest Ecology and Management

journal homepage: www.elsevier.com/locate/foreco

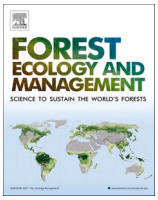

Prescribed and natural fire help restore fire-adapted conditions in an Eastern Sierra Jeffrey pine forest

Paige V. Kouba [a,*,1], Andrew M. Latimer [a], Derek J.N. Young [a], Maxwell Odkins [b], Dawson M. Bell [c], Ian R. Clark [a], Malcolm P. North [a,d]

[a] University of California, Davis, Department of Plant Sciences, One Shields Avenue, Davis, CA 95616, United States
[b] California Department of Forestry and Fire Protection, 715 P Street, Sacramento, CA 95814, United States
[c] Sonoma State University, Department of Biology, 1801 East Cotati Avenue, Rohnert Park, CA 94928, United States
[d] US Forest Service, Pacific Southwest Research Station, Davis, CA 95618, United States

ARTICLE INFO

Keywords:
Dendrochronology
Eastern Sierra
Forest reconstruction
ICO pattern
Jeffrey pine
Reference condition
Restoration

ABSTRACT

In the western US, restoring forests to historical, fire-adapted conditions can reduce fire risk, but most fire-adapted restoration targets in California focus on the western slope of the Sierra Nevada mountain range. By comparison, Eastern Sierra Jeffrey pine forests experience distinct climate and growing conditions, and both their historical structure and the effects of fire suppression are different from those of their west-side counterparts. In this study, our goals were (1) to use spatially-explicit forest reconstruction methods to estimate the historical, fire-adapted structure of eastern Sierra Jeffrey pine forests; (2) to describe the structural changes observed after 54–65 years of fire exclusion; and (3) to quantify the structural effects and restoration potential of 1–2 recent fire events that followed the fire exclusion period. At two sites in the Eastern Sierra near Mammoth Lakes, CA, we surveyed stands and collected tree ring series to establish tree ages and reconstruct maps of the forest at the end of the frequent-fire period (1941), after the period of fire exclusion (1995/2006), and in recent years (2018). We found that half a century of fire exclusion led to denser stands with fewer, smaller openings and larger clumps of trees, much like in the western Sierra. However, east-side forests were not as departed from fire-adapted conditions, and 1–2 fire events in recent years showed potential to restore many structural characteristics to their prior state. Our results can inform forest management decisions, and they support the use of prescribed fire and managed wildfire in forest restoration.

1. Introduction

In many dry conifer forests of the western US, fire exclusion has led to dramatic changes in forest structure and forest-fire feedbacks over the past century. Throughout California's history, dominant fire management practices have changed drastically due to socioecological transitions (e.g. Native American depopulation), leading to marked changes in fire regime (Taylor et al., 2016). Natural and anthropogenic fire once maintained heterogeneous forests with low tree density and surface fuel accumulation, and a high proportion of fire-adapted species like Jeffrey pine (*Pinus jeffreyi*) (Safford and Stevens, 2017). By contrast, modern California forests often have higher tree density, smaller trees, more even age classes and more shade-tolerant, less fire-adapted species (Dolanc et al., 2014, McIntyre et al., 2015, Safford and Stevens, 2017). In addition to these well-documented changes on the landscape, fire exclusion also changes within-stand spatial structure, particularly the distribution of **i**ndividual trees, tree **c**lumps, and **o**penings—hereafter ICO, (Larson and Churchill, 2012).

Fine-scale forest structural patterns are important to ecosystem functions such as drought resistance (Ma et al., 2023), habitat quality (Larson and Churchill, 2012), snow retention (Churchill et al., 2013, Stevens, 2017), fire resilience (Koontz et al., 2020), and inter- and intraspecies interactions, e.g. competition, facilitation, spread of disease, and recruitment (Larson and Churchill, 2012). Jeffrey pine in particular requires relatively large forest openings for regeneration, as seedlings need sufficient light and soil resources to grow (Gucker, 2007, Safford and Stevens, 2017). Furthermore, restoring forests to the ICO pattern they maintained prior to fire exclusion can help them support

* Corresponding author.
E-mail address: pkouba@ucsc.edu (P.V. Kouba).
[1] University of California, Santa Cruz, Department of Ecology & Evolutionary Biology; 130 McAllister Way, Santa Cruz, CA 95060.

https://doi.org/10.1016/j.foreco.2025.123010
Received 31 January 2025; Received in revised form 13 July 2025; Accepted 14 July 2025
Available online 25 July 2025

and adapt to frequent, low-intensity fire (Fry et al., 2014). Management recommendations for fuel reduction and ecological restoration in Jeffrey pine forests must therefore account for ICO patterns if they are to create meaningful restoration targets. As fine-scale site features like local climate and topography have been shown to affect the arrangement of ICO patterns within a forest (Ng et al., 2020), those targets must be attuned to local and regional influences, such as the unique climate and fire regime that distinguish the Eastern Sierra from the range's more mesic western slope (North et al., 2009)

Identifying historical ICO patterns specific to frequent-fire forests in the Eastern Sierra can help characterize the modern forest's departure from fire-adapted conditions in this area, and help set practical management and restoration targets. For example, the Eastern Sierra Climate and Communities Resilience Project is an ambitious 20-year management effort to restore fire-resilient landscapes in the 23,500 ha forest belt surrounding Mammoth Lakes, the largest population center in the Eastern Sierra (Pusina et al., 2023). Such projects must consider the spatial structure of a fire-adapted forest to achieve their goals, but Eastern Sierra forest managers have previously been forced to rely on studies from the Western Sierra to develop restoration and fire risk reduction targets (North et al., 2009).

Where they have taken place (Stanislaus Tuolumne National Forest (Lydersen et al., 2013), the Eastern Cascades (Churchill et al., 2017), Northern Arizona (Sánchez Meador et al., 2011)), forest reconstruction studies have often been limited by the long span of years elapsed since the start of fire exclusion (Lydersen et al., 2013), as early as the 1860s in most parts of the Western Sierra (Taylor et al., 2016). However, fire scar data from our study area in the Eastern Sierra record widespread forest fires until as late as 1950 (North et al., 2009). A more recent end to the frequent-fire period here has given less time for fire exclusion to influence forest structure, although main structural variables are still mostly outside the historical natural range of variation (NRV) (Meyer et al., 2019). Nonetheless, the more recent end to frequent fire suggests that standard methods of forest reconstruction can be applied with greater confidence in this setting. Identifying the spatial characteristics of the area's forests during the frequent-fire period provides a target structure for a more fire-adapted forest in the Eastern Sierra.

It is uncommon for forest reconstruction studies to examine the effects of fire's return, in addition to the effects of fire exclusion. Our study comprises three reference years (two reconstructed, one observed) to characterize forest conditions (1) during the active fire period, (2) after half a century of fire suppression, and (3) after the return of fire to the landscape. Our objectives are (1) to use forest reconstruction methods to estimate the historical, fire-adapted structure of eastern Sierra Jeffrey pine forests; (2) to describe the structural changes observed after 54–65 years of fire exclusion; and (3) to quantify the structural effects of 1–2 recent fire events that followed the fire exclusion period. In particular, we address whether fire exclusion has affected Eastern Sierra forests in the same way and to the same extent as Western Sierra forests, with the aim to inform management restoration guidelines for a greater range of frequent-fire forest types. We hypothesized that the drier, less-productive Eastern Sierra would exhibit less extreme departure from fire-adapted conditions than the Western Sierra, and that in turn that the potential restoration impact of fire return would be high.

2. Methods

2.1. Overview

We use tree ring series to develop an age-size regression model specific to our study area, and map the positions and estimated sizes of trees present before the end of frequent fire there in the mid-20th Century (frequent-fire reference year: 1941). Using the same methods, we reconstruct forest conditions immediately before the return of fire to the area (fire-excluded reference year: 1995 and 2006, respectively, at our two sites). Finally, we use observed modern forest conditions from our survey (modern reference year: 2018). We calculate metrics of historical, fire-excluded, and modern forest conditions such as tree density, basal area, and size distribution, and examine how the distribution and characteristics of individuals, clumps, and openings changed over the three time points.

2.2. Study sites

Study plots were selected in August 2018, in the Inyo National Forest on the eastern slope of the Sierra Nevada, near Mammoth Lakes, California, and within the rain shadow of the mountain range (Taylor, 1982). Three 1-ha circular plots were randomly chosen at each of two sites: Indiana Summit (IS), at the Indiana Summit Research Natural Area (ISRNA, 37.798247, −118.916090); and O'Harrell Canyon (OH), about 1.5 km northeast of the O'Harrell Canyon Creek Campground (37.757000, −118.746710) near Glass Mountain. The two sites are separated by appx. 15 km, and share a dominant vegetation type of Jeffrey pine forest (*Pinus jeffreyi* Balf.), which makes up 99.3 % of the canopy in our IS sites. OH trees were 59.6 % *P. jeffreyi*, with 19.7 % Sierra juniper (*Juniperus grandis*), 15.3 % white fir (*Abies concolor*), and 5.4 % lodgepole pine (*Pinus contorta*). Both sites are old growth/mature forests, as documented in the site history of the ISRNA (Taylor, 1982, Meyer et al., 2019) and as indicated by a lack of extractive land use history at O'Harrell Canyon (likely due to the remoteness and steep slope of this site). The O'Harrell Cayon site features no cut stumps, which characterize previously logged landscapes in this area with slow decomposition. Forests in the area are characterized by low recruitment rates and long regeneration times (Taylor, 1982), and we observed little to no understory vegetation during our surveys in 2018. Plot elevation ranged from 2571 m–2615 m at IS, and 2459 m–2559 m at OH. The dominant soil types at the sites are vitrandic xerorthents (well-drained, nutrient poor, sandy soils of volcanic origin) (USDA Soil Survey n.d.).

Fire reconstruction studies from the area determined a mean historic fire interval of 4.8–16.9 years (North et al., 2009) and 2–17 years (Brown et al., 2010), more frequent but overlapping with the estimate of an 11–16 year interval for this forest type in the Eastern Sierra as a whole prior to European settlement (Van de Water and Safford, 2011). Natural ignitions were frequent, as the area has one of the highest lightning strike rates in the state (Wagtendonk et al., 2018). Prior to European settlement, and to a lesser extent in the 20th Century, the Bishop Paiute and Mono Lake Kutzadika'a (Northern Paiute Tribes) also practiced cultural burning in the area, including as part of a process to harvest and/or prepare the larvae of the Pandora moth (*Coloradia pandora*) as a food source (Taylor, 1982, De Foliart, 2002, Slaton et al., 2019). The forests around our study sites experienced frequent fire conditions from at least the late 18th Century until ca. 1950 (North et al., 2009). The middle of the 20th Century marked the start of an era with no wildfires recorded (Taylor, 1982, North et al., 2009), with the exception of one lighting ignition in 1986, which was quickly suppressed (Slaton et al., 2019) and did not affect our study plots. It was not possible to reconstruct a timeline of fuel loading in the area with our current study methods, though fuels likely accumulated at levels higher than the NRV during the fire exclusion period. It is possible therefore that extra fuels led to more intense fire than NRV initially, upon re-introduction of fire (Hessburg et al., 2005).

Prescribed burn treatments took place between 1996–1998 in the northeast corner of ISRNA (Meyer et al., 2019), where our three 1-ha plots are located. Wildfire returned to the area in 2016, when the Clark Fire burned 99 % of the RNA (Slaton et al., 2019), including our plots. The area of the prescribed burn treatment burned at low to moderate severity in 2016, with a composite burn severity of 20 % (based on percent loss of basal area, tree density, and canopy cover after the fire) (Meyer et al., 2019). While less historical detail is available for O'Harrell Canyon (Site OH), we assign the same date for the end of the frequent-fire period there as for IS, because the three nearest sites with fire history reconstructions all record fires into the mid-20th Century,

and all three are approximately as close to OH as to IS (North et al., 2009). We were unable to find records of fire history at the O'Harrell Canyon site until 2007, when the O'Harrell Fire burned the area containing our plots at moderate severity (California Department of Forestry and Fire Protection, 2019). For a conservative estimate of the fire-adapted forest condition (i.e., the structure that existed before fire exclusion began), we chose 1941 as the focal year for our reference condition forest. We compare the reconstructed forests from 1941 to the reconstructed fire-excluded forests (1995 at IS, 2006 at OH) and the observed forests in 2018.

2.3. Sampling methods

For each plot, we recorded position, decay class, species, and diameter at breast height (DBH) for every tree and standing snag ≥ 5 cm DBH. Downed logs were measured at their maximum diameter (used to represent DBH), and the resting place of their larger end was recorded as the tree's position. In total, we recorded 1152 trees, logs, and snags across both sites. In addition, we cored 227 trees total using 4.3 mm increment borers (Haglöf, Inc.; Långsele, Sweden), at the lowest possible coring heights, ranging from 7–103 cm (average: 41.3 cm). For *P. jeffreyi*, the dominant species, we used a stratified random sampling technique to collect approximately 10 cores in each plot for each of three size classes: < 50 cm DBH, 51–90 cm DBH, and > 91 cm DBH. The > 91 cm size class sample was completed in August of 2019 at IS, and in May of 2021 at OH. Cores for *A. concolor* and *P. contorta* were collected from OH in June 2023. Attempts to core specimens of *J. grandis* failed due to the presence of rotten heartwood.

2.4. Tree core processing

Sampled cores were sanded following standard dendrochronological methods (Stokes, 1968, Speer, 2010) and scanned at 1200 dpi (EPSON WorkForce 7610 scanner), and the images were processed with CooRecorder version 7.9 (Larsson, 2005) to establish ring-width series. For most cores, the pith correction tool available in CooRecorder was used to calculate the distance to pith and the estimated number of growth years represented by said distance (based on innermost ring curvature observed in the core). Forty-one rotten or unreadable cores were excluded from the sample, yielding a total of 186 cores used to conduct dendrochronological analysis (at IS, $n = 88$, 83.0 % of cores collected; at OH, $n = 98$, 81.0 %).

Crossdating was conducted using CDendro version 7.9 (Larsson, 2005) and the dplR package in R (Bunn et al.,2024) to establish the length in years of each tree ring series. In dendrochronological analysis, a correction is necessary to account for the years of growth before the tree reached the height at which the core was taken. This core-height correction uses species-specific equations, and we used the correction equations available in the literature that most closely matched our focal species (Gascho Landis and Bailey, 2006, Fraver et al., 2011, Tomiolo et al., 2016). Since *Abies concolor* is a shade-tolerant species with highly variable growth rates at the seedling and sapling stages, no core height correction was used for this species, and tree age was recorded as the number of years observed at coring height, following Taylor and Halpern (1991).

2.5. Stand reconstruction

We used linear age-size regressions to reconstruct tree ages in 1941, before the end of the frequent-fire period. Establishing the relationship between DBH and age allowed us to extrapolate the ages (and therefore establishment dates, and ages in 1941) for all 1152 trees in the study. Trees were either assigned an age derived from their respective core sample ($n = 157$) or an age estimate from the age-size regression model ($n = 995$). For *P. jeffreyi*, we created separate age-size regressions for IS and OH, since their distinct topography and aspect were considered likely to cause different growth rates. For model selection, we compared corrected-AIC (Akaike's Information Criterion) and BIC (Bayesian Information Criterion) values (Sakamoto et al., 1986) for first- to fifth-degree polynomials of DBH as a predictor variable; in cases where AICc and BIC were not in agreement, we picked the more parsimonious model, since over-fitted models would perform poorly at predicting age from DBH. Age-size regressions for *A. concolor* and *P. contorta* were established using cores from OH only, since these species represented ≤ 0.8 % of the trees sampled at IS in 2018 (and 0 % of live trees). All models were first-degree polynomials, except for *P. contorta*, which was quadratic.

Standing snags and fallen logs ≥ 5 cm DBH were given the same diameter-based age estimate as live trees, with an additional correction for the estimated time since tree death, in order to determine their establishment dates. Time-since-death was assigned based on visually estimated decay classes (Cline et al., 1980, Stephens and Moghaddas, 2005), which we used to populate a Leslie matrix of transition probabilities between decay classes using previously published data on progressive decay in western conifers and Sierra Nevada pines (Morrison and Raphael, 1993, Kueppers et al., 2004, Edelmann et al., 2023). A full description of the methods used to assign ages for snags and logs is available in the Supplement.

Using the establishment dates determined for each tree, snag, and log, we calculated their ages as of 1941 (for the frequent-fire reference year) and the site-specific fire-excluded reference year. We removed from the dataset any trees that established after the relevant year from the dataset. Next, the reverse of the age-size regression method above was applied to the trees' past ages, to determine DBH in past reference years. We removed any trees whose size fell below 5 cm DBH. The DBH distributions of these reconstructed forest datasets were used to calculate non-spatial metrics (trees per hectare, stand density index (SDI) (Reineke, 1933), quadratic mean diameter (QMD), mean DBH, and basal area (BA)) for the forest in past reference years. A *t*-test was used to compare each of these metrics between 1941 and fire-excluded conditions, and between fire-excluded and 2018, to establish changes in plot-level and landscape-scale characteristics. Because comparisons of reconstructed stands at IS and OH revealed each site to have unique variance in initial tree size distributions, we chose to analyze changes in mean DBH on a per-site basis (IS separate from OH). For plot-level metrics, values at both sites were combined to increase statistical power.

2.6. Spatial analyses

Using the stand maps of live trees from 2018, and reconstructed maps of live trees from 1941 and the fire-excluded year at each site, we assessed forest structure in each time period, including the distribution of individual trees, clumps of trees, and openings between trees. We followed published clump detection algorithm methods (Plotkin and Muller-Landau, 2002, Churchill et al., 2017). Allometries for crown projections came from Gill et al. (2000); *P. jeffreyi* and *J. grandis* were not included in their dataset, but we used equations for the most closely related species available (*Pinus ponderosa* and *Calocedrus decurrens*, respectively). Snags and logs observed in 2018 could be used retrospectively, to reconstruct the living trees they had once been, but our methods did not provide a failsafe way of assessing snags and logs in past timesteps, as these may have been destroyed by fire. For the current study, to maintain relevant comparisons of forest structure, we therefore left standing dead wood out of the spatial analyses for both reconstructed and observed forest datasets.

Tree clumps were defined as groups of trees with overlapping crowns; a tree whose crown did not overlap with any other tree was designated an individual (representing a "clump size" of 1). The 1-ha plot boundary was corrected by a buffer inward from the plot edge, to minimize bias towards small clumps due to "truncated" clumps at the plot edge. Any stem within the buffer was counted as a clump member, but could not form the center of a new clump. Since the average crown

diameter across all plots, irrespective of time, was 4.59 m, we chose a buffer of 5 m from the plot edge, which would prevent most edge trees (trees within the buffer) from being counted incorrectly as individuals due to "invisible" out-of-bounds neighbors (Lydersen et al., 2013, Fry et al., 2014, Ng et al., 2020).

Clumps of trees and individual trees are surrounded by non-canopy area (i.e. all area in the plot not under a tree canopy), and non-canopy area is further divided into interstitial space and "openings" large enough to represent an ecologically significant interruption of the forest canopy. Openings were identified in our study using the bi0m3trics/patchwoRk package in R (Sánchez Meador, 2024), an application of the PatchMorph patch delineation algorithm (Girvetz and Greco, 2007). PatchMorph applies a circular kernel, based on user-defined parameters, to a landscape of mixed "suitable" and "unsuitable"-classified patches, delineating areas that function as suitable. Originally created for detecting habitat patches sufficient to support wildlife, the algorithm is equally well suited to defining ecologically relevant canopy openings within a forested area (Lydersen et al., 2013, Fry et al., 2014, Ng et al., 2020).

The resulting ICO distribution datasets were used to statistically compare the stand structure of the forest at the end of the frequent fire period (1941); at the end of the fire exclusion period (1995 at IS, 2006 at OH); and in modern times, after 1–2 fires had returned (2018).

We used Fisher's exact test to compare the number of tree clumps observed for each clump size between the three reference years (from 2–15 trees per clump at IS; 2–18 at OH; and with individual trees counted as "one-tree clumps"), providing an estimate of the degree of overall forest structural change at each site. To find changes specific to individuals and binned clump sizes, contingency analysis of binned structural categories was performed, aggregating both IS and OH and using Fisher's exact test with a Bonferroni correction due to multiple tests (significance threshold of $p < 0.0125$). Bins included individual trees (1-tree "clumps"), and small (2–4 trees), medium (5–9), and large (10 +) clumps (Lydersen et al., 2013, Churchill et al., 2017). We compared the distribution of binned forest openings and binned clumps at both sites in all three reference years using permutational multivariate analysis of variance (PERMANOVA), with "Plot" as a blocking variable due to repeated measures. Gap-size bins were 82–500, 500–1500, 1500–2500, and > 2500 m^2. Data processing and statistical analyses were performed in R (4.2.2) using the dplR, patchwork, spatstat (Baddeley et al., 2024), sf (Pebesma et al., 2024), terra (Hijmans et al., 2024), and vegan (Oksanen et al., 2024) packages.

3. Results

3.1. Age-size regressions

The final age-size regression models for *P. jeffreyi* at IS and OH had R^2 values of 0.653 and 0.646, respectively (n = 88 for *P. jeffreyi* at IS, $p < <.001$; n = 79 for *P. jeffreyi* at OH, $p < <.001$). The age-size regression for *A. concolor* had an R^2 of 0.514, and the regression for *P. contorta* had an R^2 of 0.798 ($n = 10$ for *A. concolor*, $p = 0.02$; $n = 9$ for *P. contorta*, $p = 0.003$).

Table 1
non-spatial metrics of forest density and tree size.

Variable	Units	Description
TPH	trees ha^{-1}	Density of stems per hectare
SDI	–	Stand density index
QMD	cm	Quadratic mean diameter
mean DBH	cm	Arithmetic mean diameter
BA	m^2 ha^{-1}	Total basal area of stems per hectare

3.2. Non-spatial forest structure metrics

Average live tree DBH showed no change for the first period analyzed here (i.e. between 1941 and the fire-excluded reference year) (IS, $p = 0.32$; OH, $p = 0.17$), a period of 54–65 years (Fig. 1). The number of trees per hectare (TPH) across both sites increased significantly in the same period (from 70 to 133 trees, $p = 0.03$). Basal area (BA) across both sites increased significantly (from 11.9 to 22.6 m^2 ha^{-1} [51.8–98.4 sq ft per acre], $p = 0.0003$). Stand density index (SDI) increased significantly from 73.9 to 141.5 ($p < 0.001$). While IS was nearly a pure *P. jeffreyi* stand in all three reference years (with single-digit numbers of *P. concolor* the only exception), OH exhibited more species diversity overall, and a shift towards more shade-tolerant species during the fire exclusion period. In the 1941 forest reconstruction for OH, we found that *P. jeffreyi* made up 86.1 % of the live trees, with only 3.1 % *A. concolor* and 10.6 % *J. grandis*. The fire-excluded condition there (2006) featured 63.8 % *P. jeffreyi* in the live-tree canopy, with 11.2 % *A. concolor* and 20.7 % *J. grandis* (the remainder *P. concolor*).

For the second period of analysis (i.e. between the fire-excluded reference year and the modern forest), we made similar comparisons between metrics. Over this 12–23-year period (which included 1–2 fires), average live tree DBH increased significantly at IS (+13.8 cm [5.4 in], 95 % CI 9.9–17.7; $p < <.001$), while at OH it did not change ($p = 0.39$). IS also exhibited a marginally significant increase of approximately 35 % in QMD for this period (treated as a plot-level variable, $p = 0.05$). The change in TPH across both sites was negative but not significantly so ($p = 0.13$). Basal area did not change significantly ($p = 0.77$) and was the only metric that showed opposite signs at either site for this time period (slight increase at IS, decrease at OH). SDI decreased, but not significantly (141.5–129.1; $p = 0.46$).

3.3. Spatial patterns

The clump detection algorithm allowed a comparison of individuals, clumps, and openings at each site and across both sites during the fire exclusion period (Fig. 2a and b). At IS, average clump size increased from 1.45 to 2.53 trees, an increase of 1.08 trees ($p < <.001$). At OH, average clump size increased from 1.29 to 1.96 trees, an increase of 0.67 trees ($p < <.001$). Across both sites, the average clump size increased from 1.38 to 2.26 trees (+0.88, $p < <.001$).

The proportional area belonging to each structural category shows a shift toward larger clump sizes, and away from individual trees and openings, for each site during the fire exclusion period (Fig. 3). At each site, the most notable change in structural categories on a per-area basis was the decreased area in openings (-18.2 % at IS, −24.9 % at OH).

From the end of the fire exclusion period to the modern forest, average clump size did not change significantly at either site (IS, $p = 0.48$; OH, $p = 0.79$), nor for both sites pooled together ($p = 0.36$). The average proportion of plot area in forest openings increased by 10.7 % at IS and 2.9 % at OH during this period.

3.4. Changes in distribution of individuals, clumps, and openings

The change in the overall frequency distribution of individuals and tree clumps of all sizes was highly significant at both sites from 1941 to the fire-excluded reference years ($p < 0.001$ at IS, $p = 0.03$ at OH), but not from the fire-excluded years to 2018 ($p = 0.94$, 0.92) (Table 2). Binned forest openings, combined between sites, shifted towards smaller sizes in the fire-exclusion period; their distribution was marginally different between the two reference years ($p = 0.06$) (Fig. 4). The distribution of counts per hectare for all structural categories (binned gaps (Fig. 4) and binned cluster sizes (Fig. 5)) also changed significantly from 1941 to the fire-excluded year ($p = 0.03$).

From 1941 to the end of the fire exclusion period, the proportion of trees that were individuals decreased from 55.2–24.0 % at IS, and from 62.0–34.4 % at OH. Contingency analysis of binned clump sizes across

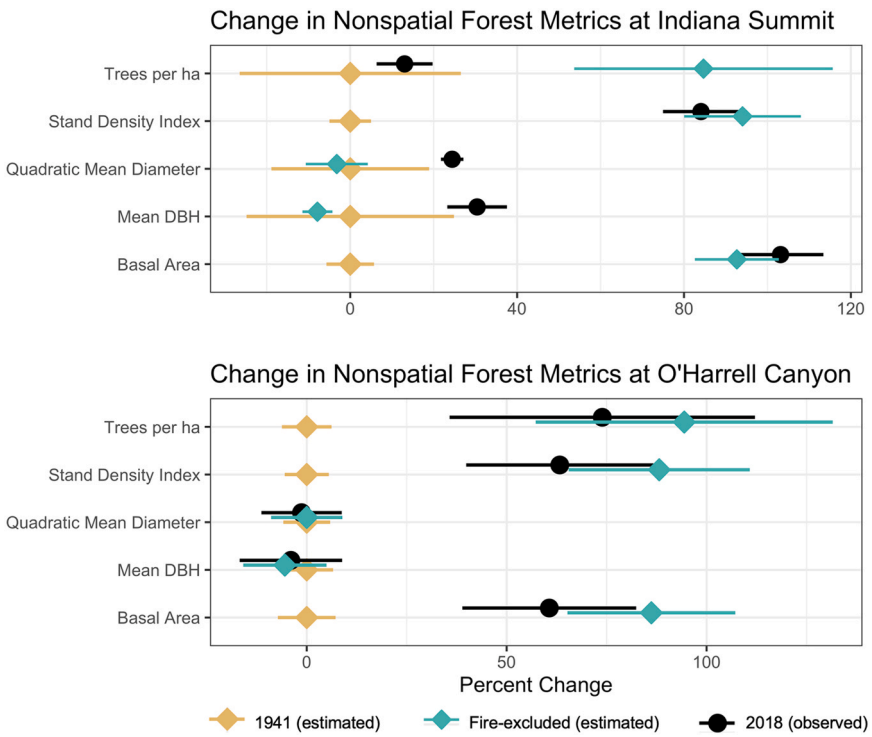

Fig. 1. Mean percent change in non-spatial forest metrics at Indiana Summit and O'Harrell Canyon. 1941, the frequent-fire reference year, represents the baseline, with fire-excluded and modern conditions shown as percent change. Between the fire-excluded period and 2018, Indiana Summit experienced two fires (in 1996 and 2016), and O'Harrell Canyon experienced one (in 2007). Error bars represent standard error across three plots per site.

both sites revealed a highly significant change in the proportions of all but one structural category from 1941 to the end of fire exclusion: a decrease in the proportion of tree clumps that were individuals (76.5–58.3 %, $p < <.001$); an increase in small (2–4 tree) clumps that did not meet the

threshold for statistical significance (22.8–33.9 %, $p = 0.29$); an increase in medium (5–9 tree) clumps (0.3–9.1 %, $p < <.001$); and an increase in large (10 + tree) clumps (0.3–2.3 %, $p < <.001$).

While there was a shift toward less total area in openings during the fire-exclusion period, the average number of openings per hectare increased (from 4.3 to 5.2). The average gap size across both sites decreased by over half (from 1086 m^2 to 493 m^2), although this change was only marginally statistically significant ($p = 0.07$).

From the end of the fire-exclusion period until 2018, none of the clump sizes showed a significant change. The average openings per hectare decreased from 5.2 to 3.5, though not achieving statistical significance ($p = 0.13$). The overall change in the distribution of binned forest openings was not significant ($p = 0.31$), but the change in distribution of counts per hectare for all structural categories was marginally significant for this period ($p = 0.06$). However, the average gap size in 2018 was 1014 m^2, and mean gap size was not significantly different from mean gap size in the original 1941 forest (1087 m^2, $p = 0.87$).

4. Discussion

4.1. Overview

Our results show that 54–65 years of fire exclusion in an Eastern Sierra Jeffrey pine forest led to denser stands with fewer, smaller openings and larger clumps of trees. The changes observed were aligned with trends in more mesic Western Sierra mixed conifer forests, with two exceptions: (1) average DBH did not significantly decrease in our study system, as it has across much of the Western Sierra in fire-excluded stands; (2) the fire-excluded forest in our study had much lower average cluster size than fire-excluded West-side forests. Comparing the fire-excluded forests to the 2018 condition, after 1–2 fires, we found that the return of fire to the landscape had partially reversed the changes that occurred during the fire exclusion era.

4.2. Frequent-fire to fire-excluded period (1941–1995/2006)

Increases in average clump size, more area in large clumps, and less area in gaps is consistent with changes observed in fire-excluded Western Sierra forests (Lydersen et al., 2013) and with comparisons to a different old-growth Jeffrey pine forest in Northern Mexico (Fry et al., 2014). Our site, however, had about twice the proportion of individual trees as these western Sierran and northern Mexican analogues, and only one-fifth to one-third as many trees in large clumps. We compared our Fire-Exclusion dataset with Lydersen et al.'s 1929 and Fry et al.'s northern Mexico sites, because the fire exclusion period for each was 40 and 68 years, comparable to our 54–65. The changes in average gap size and gap size distribution was pronounced during the period of fire exclusion, but it was neither the most nor the least extreme result and they fell somewhere in between the extremes among studies on Western forest reference conditions. On the West slope of the Sierra, the era of fire suppression all but erased forest openings from the landscape in many areas (although typically this change took two to three times longer than the half-century of fire exclusion experienced at our sites) (Lydersen et al., 2013). By contrast, Fry et al. found no significant difference in gap size distribution between fire-adapted *P. jeffreyi* forests in northern Mexico and their fire-suppressed Sierra comparison sites. Although we observed an increased density of stems and increased average clump size during the fire-exclusion period, a slower rate of growth, dry conditions, and predominance of shade-intolerant species mean eastern Sierra forests are less departed from frequent-fire conditions than their west-side counterparts. The consistent average DBH may also be in part due to the lack of logging activity in our study area, as logging tends to remove the largest trees. Our findings for this period were in agreement across both our study sites (IS and OH).

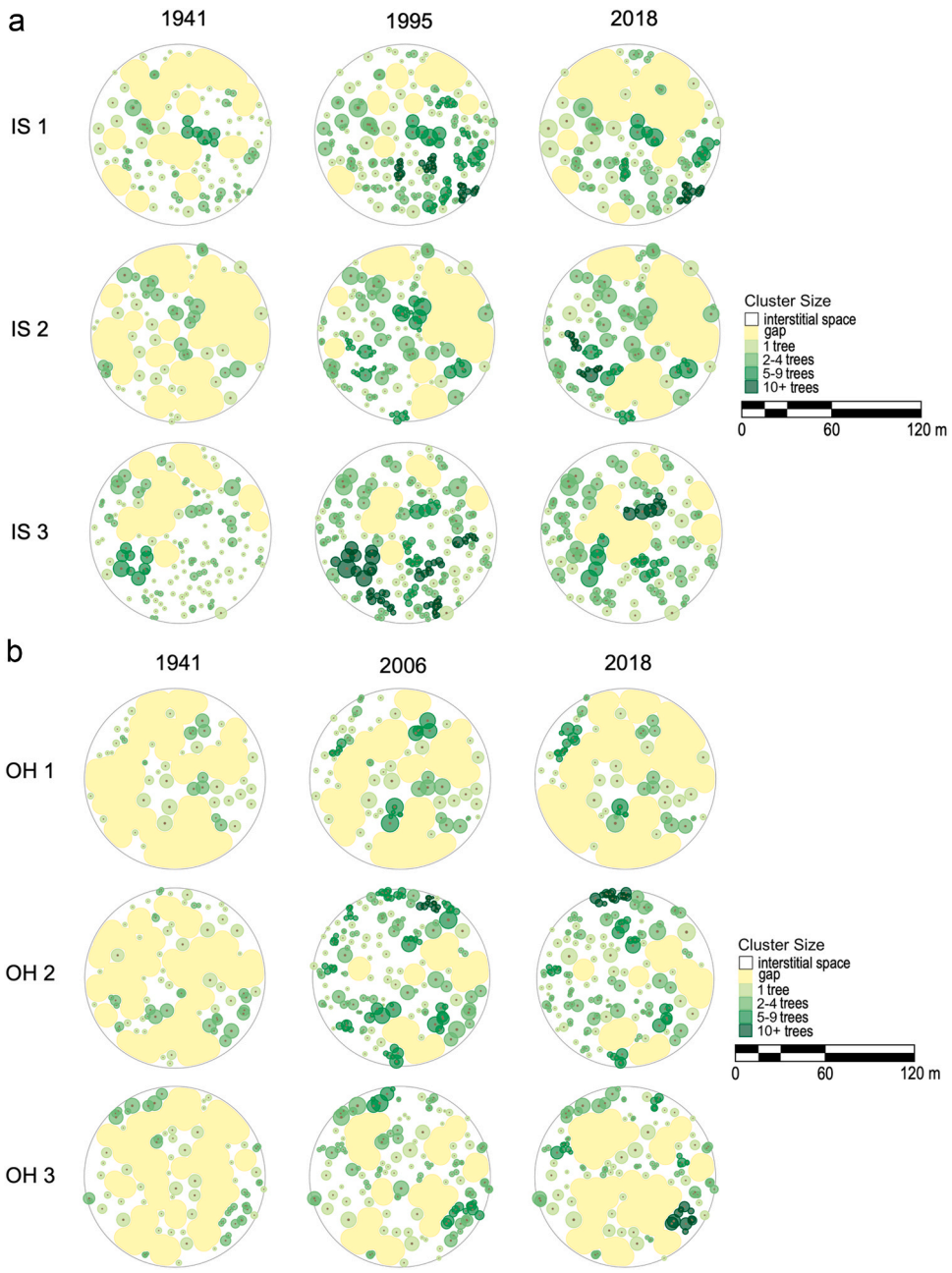

Fig. 2. Top-down maps showing crowns and stems of living trees at Indiana Summit (2a) and O'Harrell Canyon (2b). Columns show the frequent-fire reference year (1941, reconstructed); fire-excluded reference year (1995 at IS and 2006 at OH, reconstructed); and the modern reference year (2018, observed). Each plot (rows) is 1 ha in size.

Although our study featured areas dominated by *P. jeffreyi*, a lack of fire led to a slight change in species composition, at least at one of our two sites, to include more *A. concolor* after a period of fire exclusion. This finding is consistent with observations across Western U.S. forests, that fire-suppressed forests feature higher proportions of shade-tolerant trees like *A. concolor* compared to frequent fire forests (McIntyre et al., 2015, Safford and Stevens, 2017).

4.3. Fire-excluded to modern period (1995/2006–2018)

Our results also indicate that the structural characteristics of a fire-adapted Eastern Sierra forest have been partly restored since fire returned to this landscape, especially at the site which burned twice, at moderate severity, in the last 23 years (IS). We examined the spatial and structural changes caused by the return of prescribed and/or wildfire to the landscape, by comparing the fire-excluded forest to the forest in 2018. We found that both sites recovered some of the losses to their total area in openings, using the 1941 forest as the baseline: 58.8 % for IS, and 11.6 % for OH. Meanwhile, average opening size was restored to 1941 levels at both sites. Average gap size and total gap area have different ecological impacts and are both useful metrics for restoration management.

The sites differed in the trends in their average stem density and tree size: while OH saw a modest recovery of TPH (about 20 % restored to 1941 values), and had no significant change in average DBH during the fire-return period, IS, in contrast, had almost full recovery of 1941 live stem density, and an increase in mean DBH. This difference between the two sites is likely due to the fact that IS had burned twice since the end of the fire exclusion period, and had burned more recently by the time we gathered the 2018 data (two years prior, vs. 11 years at OH). In fact,

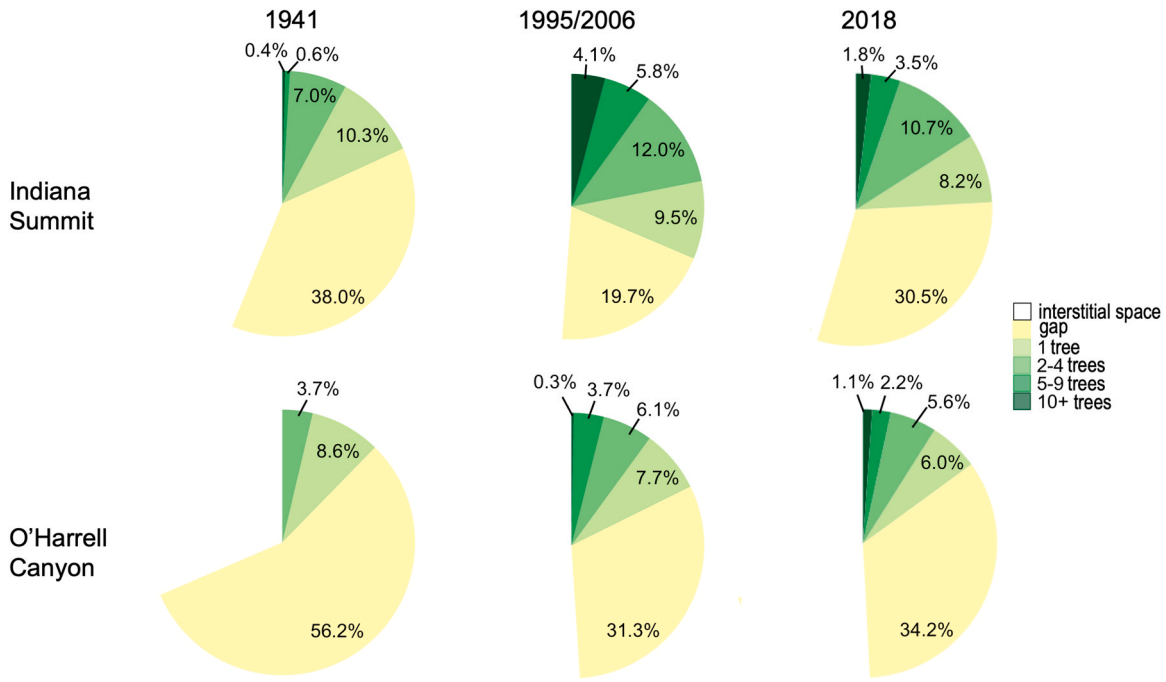

Fig. 3. Proportion of forest area in each structural group: individuals; small (2–4 tree), medium (5–9 tree), and large (10 + tree) clumps; and interstitial space. At each of the two sites (Indiana Summit, top row; O'Harrell Canyon, bottom row) we surveyed three 1-ha plots, which have been aggregated for this analysis. Columns show the frequent-fire reference year (1941, reconstructed); the fire-excluded reference year, one year before the return of fire (1995 at IS and 2006 at OH, reconstructed); and the modern reference year (2018, observed).

56.2 % of the increase in mean DBH at IS can be attributed to removal of the Class 1 snags ($n = 181$, mean DBH 21.1 cm) from the live tree population by the 2016 Clark Fire. These two cases suggest the utility of multiple burns in restoring fire-adapted forest structure, and we caution that the severity of the fires in question is also important. Our study plots at IS were burned in a prescribed fire treatment between 1996–1998, and reburned at low-to-moderate severity in the 2016 Clark Fire. *Outside* the prescribed burn area from the 1996–1998 treatments, 36 % of ISRNA burned at high severity, and sustained much higher mortality (Meyer et al., 2019). OH, which had lower stem density and fuel loads compared to IS at the time of fire return, burned at moderate severity during its first fire event after the fire exclusion period, despite having had no prior thinning or prescribed burning. In low-density areas, and barring extreme fire weather, managed natural fire can begin the work of restoring fire-adapted stand structure. However, if dense, fire-excluded forests are exposed to high severity fire without any pre-treatment, fire is unlikely to help restore reference conditions, and may instead cause enough mortality to put large areas of the forest at risk of regeneration failure (Meyer et al., 2019). Future work could identify specific thresholds of prescribed fire severity and frequency that best achieve the restoration effects observed in this study.

4.4. Limitations

The methods of our study feature a number of limitations which may affect the interpretation of our results.

To reconstruct historical forest conditions and understand the effects of fire exclusion followed by reintroduction, our study required old-growth forest conditions which, after decades of fire exclusion, experienced a return of fire *and* burned at only low to moderate severity. Although our study took place within the largest contiguous Jeffrey Pine forest in the world, these conditions are very rare, and the spatial extent of our study area was therefore restricted. While a larger study area would improve the generalizability of our results, we note that ICO patterns are best assessed at scales 0.8 ha and above (Kane et al., 2015), and we ensured that our methods met this criteria in spite of the rarity of our focal forest type.

There are certain disadvantages to choosing presettlement conditions as a reference condition for fire-adapted forests, or any type of ecological restoration: some consider it overly prescriptive, as climate and society have changed dramatically (Urgenson et al., 2018); and past conditions may have exhibited nonequilibrium dynamics, making them less useful as management targets (Swetnam et al., 1999). Still, of the available options, spatially-explicit historical reference conditions like the ones in our study are the best-suited to testing against projected climate conditions (Churchill et al., 2013), and the most commonly used by restoration practitioners (Urgenson et al., 2018).

Over the course of the 77 years examined in our study, the slow changes brought about by fire exclusion were occurring in tandem with, and likely influenced by, changes in global climate. Atmospheric CO_2 levels have risen by about 100 ppm since then (Gulev et al., 2021), hastening both abrupt disturbances like hotter droughts, and also gradual shifts in growing conditions (USGCRP, 2018). Forest mortality in the Sierra Nevada increased twofold between 1983 and 2004 (van Mantgem and Stephenson, 2007), and forests in the southwestern United States have a demonstrated lack of regeneration due to climate-related changes in environmental stresses like soil water and temperature (Petrie et al., 2023). It is likely that during the fire exclusion period (1941–1995/2006), the increased stand density indicated in our results occurred in *spite* of climate-induced increases in mortality rates. On the other hand, the effect of fires from 1995 to 2018, restoring lower-density forests with more openings, was probably aided to some degree by climate-induced increases in mortality and reductions in regeneration.

4.5. Conclusions and management recommendations

Our study provides the first spatially-explicit evidence of fire suppression and fire return's effects on Eastern Sierra Jeffrey pine forests, which can inform management decisions in this ecosystem.

In seeking to restore frequent-fire conditions, forest managers have a number of tools at their disposal: western Sierra studies on fuels management focus on mechanical treatments, prescribed fire, and their

Table 2
Summary of characteristics, across sites and years, of individual trees; small, medium, and large clumps of trees; and stand-level structure. Figures are mean and (standard deviation). Note that "Trees/ha within clump" is a measure of tree density inside the area bounded by the canopy of the outermost trees in a clump.

		IS in 1941	IS Fire-Excluded	IS in 2018	OH in 1941	OH Fire-Excluded	OH in 2018	All in 1941	All Fire-Excluded	All in 2018
Individual Trees	# Trees/ha	45.3 (19.1)	36 (7.5)	22.7 (6.7)	34 (2)	38.7 (5)	33.7 (10.4)	39.7 (13.7)	37.3 (5.9)	28.2 (9.9)
	Proportion of trees (%)	55.2 (4.5)	24 (3.6)	24.5 (6)	62 (9.8)	37.5 (12.9)	34.4 (5.1)	58.6 (7.8)	30.8 (11.2)	29.4 (7.4)
	Mean DBH	27 (12.4)	28.7 (2.6)	46.5 (8.9)	36.9 (5.7)	33.1 (10.7)	42.7 (10.9)	32 (10.2)	30.9 (7.4)	44.6 (9.2)
	BA (sq m/ha)	3.7 (1.6)	3.3 (1.6)	5.6 (3.6)	6.3 (1.2)	6 (2.7)	7.3 (0.6)	5 (1.9)	4.6 (2.5)	6.4 (2.5)
	Proportion of plot area (%)	10.3 (1.2)	9.5 (3.1)	8.2 (3.9)	8.6 (1.7)	7.7 (2.6)	6 (2.8)	9.5 (1.6)	8.6 (2.7)	7.1 (3.2)
Small Clusters (2−4)	# Clusters/ha	15 (7)	22.3 (6.4)	17.7 (3.1)	8.7 (2.3)	16.3 (9)	15.7 (9.6)	11.8 (5.8)	19.3 (7.7)	16.7 (6.5)
	Proportion of trees (%)	40.3 (0.9)	38.8 (1.6)	45.6 (4.9)	38 (9.8)	34.6 (14.3)	38.1 (8)	39.1 (6.3)	36.7 (9.4)	41.8 (7.2)
	Mean DBH	42.8 (24.6)	38.9 (9)	51.5 (6.2)	48.2 (7.8)	44.1 (7.6)	42.9 (15.2)	45.5 (16.6)	41.5 (8)	47.2 (11.4)
	BA (sq m/ha)	7 (2.4)	11.8 (1.6)	13.6 (3)	5.2 (1.4)	9.1 (3.9)	7.2 (3.2)	6.1 (2)	10.4 (3)	10.4 (4.5)
	Trees/ha within clump	577.1 (135.9)	626 (70.6)	536.1 (123.5)	743.5 (177.3)	896.4 (270.8)	805.6 (116.1)	660.3 (168.1)	761.2 (230.8)	670.9 (182.4)
	Proportion of plot area (%)	7 (1.8)	12 (4)	10.7 (3.5)	3.7 (2.4)	6.1 (4.6)	5.6 (3)	5.3 (2.6)	9 (5)	8.2 (4)
Medium Clusters (5−9)	# Clusters/ha	0.3 (0.6)	6 (1.7)	3.3 (0.6)	0 (0)	5.7 (4.6)	3.7 (1.2)	0.2 (0.4)	5.8 (3.1)	3.5 (0.8)
	Proportion of trees (%)	2.1 (3.7)	22.3 (10.5)	17.3 (2.8)	0 (0)	25.4 (12.8)	21.3 (9.5)	1.1 (2.6)	23.8 (10.6)	19.3 (6.7)
	Mean DBH	63.4 (NA)	33.4 (3.2)	49.7 (10.4)	-	43.4 (9.7)	34.2 (8)	63.4 (NA)	38.4 (8.4)	42 (11.9)
	BA (sq m/ha)	0.9 (1.5)	6.4 (2.9)	5.7 (0.7)	0 (0)	7.4 (3.7)	3.4 (2.3)	0.4 (1)	6.9 (3)	4.6 (2)
	Trees/ha within clump	35.9 (62.1)	373.2 (212.3)	212.5 (92.8)	0 (0)	865.6 (623.1)	503.5 (362.7)	17.9 (43.9)	619.4 (496.1)	358 (285.4)
	Proportion of plot area (%)	0.6 (1)	5.8 (2.1)	3.5 (1.3)	0 (0)	3.7 (2.4)	2.2 (0.5)	0.3 (0.7)	4.7 (2.3)	2.8 (1.1)
Large Clusters (10 +)	# Clusters/ha	0.3 (0.6)	2.7 (2.5)	1.3 (0.6)	0 (0)	0.3 (0.6)	0.7 (0.6)	0.2 (0.4)	1.5 (2.1)	1 (0.6)
	Proportion of trees (%)	2.4 (4.2)	14.9 (13.8)	12.6 (5.5)	0 (0)	2.5 (4.4)	6.2 (5.4)	1.2 (3)	8.7 (11.4)	9.4 (6)
	Mean DBH	70.4 (NA)	28.9 (10.7)	35.3 (15.1)	-	15.9 (NA)	45.7 (11.6)	70.4 (NA)	24.5 (10.7)	39.4 (13.4)
	BA (sq m/ha)	1.4 (2.5)	3.8 (5.3)	1.8 (1)	0 (0)	0.1 (0.2)	1.7 (1.5)	0.7 (1.8)	2 (3.9)	1.7 (1.1)
	Trees/ha within clump	37.1 (64.3)	222.9 (199.4)	162.8 (112.3)	0 (0)	77.2 (133.6)	116.6 (105.4)	18.6 (45.5)	150 (171.5)	139.7 (100.6)
	Proportion of plot area (%)	0.4 (0.6)	4.1 (4.1)	1.8 (0.3)	0 (0)	0.3 (0.5)	1.1 (1.2)	0.2 (0.4)	2.2 (3.3)	1.5 (0.9)
Stand	Stem density/ha	101.7 (40.5)	188.3 (4.2)	120 (10.5)	62.7 (13.3)	130.7 (54)	112.3 (49.1)	82.2 (34.4)	159.5 (54.9)	116.2 (32)
	BA (sq m/ha)	12.9 (1.6)	25.3 (1.6)	26.8 (1.4)	11.5 (0.6)	22.6 (5)	19.6 (5.1)	12.2 (1.3)	24 (3.6)	23.2 (5.2)
	Mean DBH	35.5 (15.1)	34 (3)	47.4 (2.8)	41 (4.8)	38.5 (6.7)	40.7 (7.4)	38.2 (10.5)	36.3 (5.3)	44 (6.2)
	Mean trees/cluster	1.4 (0)	2.5 (0.2)	2.4 (0.4)	1.3 (0.1)	1.9 (0.5)	1.9 (0.1)	1.4 (0.1)	2.2 (0.5)	2.1 (0.4)
	Max trees/cluster	7 (3)	12.3 (3.8)	11.7 (1.5)	3.3 (0.6)	9.3 (4.2)	11.3 (4.2)	5.2 (2.8)	10.8 (3.9)	11.5 (2.8)
	Mean gaps/ha	6 (2)	5.7 (1.5)	3.7 (0.6)	2.7 (1.5)	4.7 (1.2)	3.3 (2.1)	4.3 (2.4)	5.2 (1.3)	3.5 (1.4)

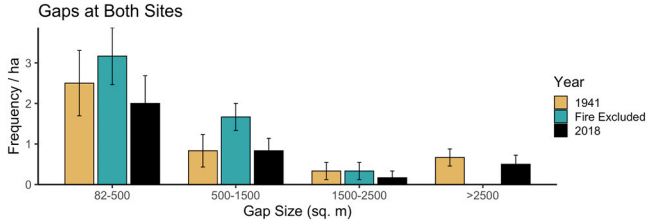

Fig. 4. Frequency distribution of forest opening size categories, expressed in square meters, averaged across Indiana Summit and O'Harrell Canyon. Bars represent standard error.

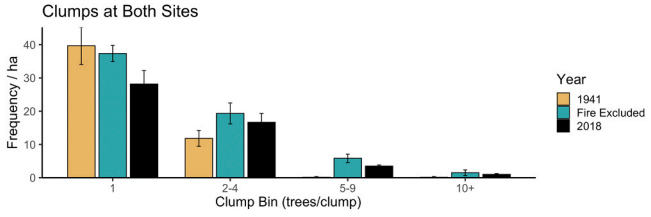

Fig. 5. Frequency distribution of tree clump size categories, in number of trees per clump, averaged across Indiana Summit and O'Harrell Canyon. Bars represent standard error.

combination, with an additional variable to account for the frequency of application for each treatment (Stephens et al., 2024, Brodie et al., 2024). Such research has found that a combination of thinning and prescribed burning is typically the most effective in moderating the effects of modeled (Stephens et al., 2024) and real-world (Brodie et al., 2024) fire return. The longevity of treatment effects depends on site productivity, suggesting that such treatments can have long-lasting effects in dry, relatively slow-growing East Sierra Jeffrey pine forests.

The Eastern Sierra Climate and Communities Resilience Project, informally known as the "Mammoth Donut," is an ambitious project that will unfold over the next 15–20 years, attempting to return the forests to a condition that can withstand both prescribed and managed natural fire (Pusina et al., 2023). As the Clark Fire at IS (outside our plot areas) demonstrated, high-severity, uncontrolled wildfire can have devastating impacts on fire-suppressed forests if they have not been treated with some level of active management in preparation (Meyer et al., 2019). Our study shows that first- and second-entry, low-to-moderate-severity fires (natural at OH, and a mix of natural and prescribed at IS) are able to partially restore historical conditions in fire-excluded forests. Along with thinning, prescribed burns and managed natural fires will be an important tool to prepare Eastern Sierra communities for fire resistance and resilience (North et al., 2012).

CRediT authorship contribution statement

Paige V. Kouba: Formal analysis, Investigation, Writing — original draft, Visualization. **Andrew M. Latimer:** Formal analysis, Supervision. **Derek J.N. Young:** Methodology. **Maxwell Odkins:** Investigation, Data curation, Project administration. **Dawson M. Bell:** Investigation, Data curation. **Ian R. Clark:** Investigation, Data curation. **Malcolm P. North:** Conceptualization, Supervision, Project administration. All authors contributed to review and editing of the manuscript.

Funding Statement

Support for this research was provided by the UC Davis Plant Sciences Department, the UC Davis Graduate Group in Ecology, the UC Davis Institute of the Environment, the Jastro Shields Graduate Research Award, and the USFS Pacific Southwest Research Station.

Declaration of Competing Interest

The authors declare that they have no known competing financial interests or personal relationships that could have appeared to influence the work reported in this paper.

Acknowledgements

We thank Adriana Postema, Jill Dyer, Emily Bell, Derek Churchill, Andrew J. Sánchez Meador, Joseph Levine, and Marc Meyer for their assistance in conducting this study.

Appendix A. Supporting information

Supplementary data associated with this article can be found in the online version at doi:10.1016/j.foreco.2025.123010.

Data availability

Data will be made available on request.

References

Baddeley, A., R. Turner, and E. Rubak. 2024, July 15. spatstat: Spatial Point Pattern Analysis, Model-Fitting, Simulation, Tests.

Brodie, E.G., Knapp, E.E., Brooks, W.R., Drury, S.A., Ritchie, M.W., 2024. Forest thinning and prescribed burning treatments reduce wildfire severity and buffer the impacts of severe fire weather. Fire Ecol. 20, 17.

Brown, P., C. Gentry, B. Cassell, A. Dugan, J. Harris, C. King, J. Marschall, D. Pérez-Salicrup, G. Smith, and J. Waldron. 2010. Fire and recruitment history of a Jeffery pine stand in the eastern Sierra Nevada, California.

Bunn, A., M. Korpela, F. Biondi, F. Campelo, P. Mérian, F. Qeadan, C. Zang, A. Buras, A. Cecile, M. Mudelsee, M. Schulz, S. Klesse, D. Frank, R. Visser, E. Cook, and K. Anchukaitis. 2024, June 1. dplR: Dendrochronology Program Library in R.

California Department of Forestry and Fire Protection. 2019, December 19. California Fire Perimeters (all). California State Geoportal.

Churchill, D., Larson, A., Dahlgreen, M., Franklin, J., Hessburg, P., Lutz, J., 2013. Restoring forest resilience: From reference spatial patterns to silvicultural prescriptions and monitoring. For. Ecol. Manag. 291, 442–457.

Churchill, D.J., G.C. Carnwath, A.J. Larson, and S.A. Jeronimo. 2017. Historical forest structure, composition, and spatial pattern in dry conifer forests of the western Blue Mountains, Oregon. Page PNW-GTR-956. U.S. Department of Agriculture, Forest Service, Pacific Northwest Research Station, Portland, OR.

Cline, S.P., Berg, A.B., Wight, H.M., 1980. Snag characteristics and dynamics in douglas-fir forests, Western Oregon. J. Wildl. Manag. 44, 773–786.

De Foliart, G.R. 2002. Insects Formerly Used as Food by Indigenous Populations of North America North of Mexico. Page The Human Use of Insects as a Food Resource. University of Wisconsin.

Dolanc, C.R., Safford, H.D., Thorne, J.H., Dobrowski, S.Z., 2014. Changing forest structure across the landscape of the Sierra Nevada, CA, USA, since the 1930s. Ecosphere 5 art101.

Edelmann, P., Weisser, W.W., Ambarlı, D., Bässler, C., Buscot, F., Hofrichter, M., Hoppe, B., Kellner, H., Minnich, C., Moll, J., Persoh, D., Seibold, S., Seilwinder, C., Schulze, E.-D., Wöllauer, S., Borken, W., 2023. Regional variation in deadwood decay of 13 tree species: effects of climate, soil and forest structure. For. Ecol. Manag. 541, 121094.

Fraver, S., J.B. Bradford, and B.J. Palik. 2011. Improving Tree Age Estimates Derived from Increment Cores: A Case Study of Red Pine:7.

Fry, D.L., Stephens, S.L., Collins, B.M., North, M.P., Franco-Vizcaíno, E., Gill, S.J., 2014. Contrasting spatial patterns in active-fire and fire-suppressed mediterranean climate old-growth mixed conifer forests. PLoS ONE 9, e88985.

Gascho Landis, A.M., Bailey, J.D., 2006. Predicting age of pinyon and juniper using allometric relationships. West. J. Appl. For. 21, 203–206.

Gill, S.J., Biging, G.S., Murphy, E.C., 2000. Modeling conifer tree crown radius and estimating canopy cover. For. Ecol. Manag. 126, 405–416.

Girvetz, E.H., Greco, S.E., 2007. How to define a patch: a spatial model for hierarchically delineating organism-specific habitat patches. Landsc. Ecol. 22, 1131–1142.

Gucker, C.L., 2007. S. department of agriculture, forest service, rocky mountain research station, fire sciences laboratory. Pinus jeffreyi. U.

Gulev, S.K., P.W. Thorne, J. Ahn, F.J. Dentener, C.M. Domingues, S. Gerland, D. Gong, D. S. Kaufman, J.Q. Nnamchi, J.A. Rivera, S. Sathyendranath, S.L. Smith, B. Trewin, K. von Schuckmann, and R.S. Vose. 2021. Changing State of the Climate System. Pages 287–422 in Intergovernmental Panel on Climate Change (IPCC), editor. Climate Change 2021: The Physical Science Basis. Contribution of Working Group I to the Sixth Assessment Report of the Intergovernmental Panel on Climate Change [Masson-Delmotte, V., P. Zhai, A. Pirani, S.L. Connors, C. Péan, S. Berger, N. Caud, Y. Chen, L. Goldfarb, M.I. Gomis, M. Huang, K. Leitzell, E. Lonnoy, J.B.R. Matthews, T. K. Maycock, T. Waterfield, O. Yelekçi, R. Yu, and B. Zhou (eds.)]. Cambridge University Press, Cambridge.

Hijmans, R.J., R. Bivand, K. Dyba, E. Pebesma, and M.D. Sumner. 2024, May 22. terra: Spatial Data Analysis.

Hessburg, P.F., Agee, J.K., Franklin, J.F., 2005. Dry forests and wildland fires of the inland Northwest USA: Contrasting the landscape ecology of the pre-settlement and modern eras. Forest Ecology and Management, Relative Risk Assessments for Decision –Making Related To Uncharacteristic Wildfire 211, 117–139. https://doi.org/10.1016/j.foreco.2005.02.016.

Kane, V.R., Cansler, C.A., Povak, N.A., Kane, J.T., McGaughey, R.J., Lutz, J.A., Churchill, D.J., North, M.P., 2015. Mixed severity fire effects within the Rim fire: Relative importance of local climate, fire weather, topography, and forest structure. For. Ecol. Manag. 358, 62–79. https://doi.org/10.1016/j.foreco.2015.09.001.

Koontz, M.J., North, M.P., Werner, C.M., Fick, S.E., Latimer, A.M., 2020. Local forest structure variability increases resilience to wildfire in dry western U.S. coniferous forests. Ecol. Lett. 23, 483–494.

Kueppers, L.M., Southon, J., Baer, P., Harte, J., 2004. Dead Wood Biomass and Turnover Time, Measured by Radiocarbon, along a Subalpine Elevation Gradient. Oecologia 141, 641–651.

Larson, A.J., Churchill, D., 2012. Tree spatial patterns in fire-frequent forests of western North America, including mechanisms of pattern formation and implications for designing fuel reduction and restoration treatments. For. Ecol. Manag. 267, 74–92.

Larsson, L.-Å. 2005. CDendro & CooRecorder program package.

Lydersen, J.M., North, M.P., Knapp, E.E., Collins, B.M., 2013. Quantifying spatial patterns of tree groups and gaps in mixed-conifer forests: reference conditions and long-term changes following fire suppression and logging. For. Ecol. Manag. 304, 370–382.

Ma, Q., Su, Y., Niu, C., Ma, Q., Hu, T., Luo, X., Tai, X., Qiu, T., Zhang, Y., Bales, R.C., Liu, L., Kelly, M., Guo, Q., 2023. Tree mortality during long-term droughts is lower in structurally complex forest stands. Nat. Commun. 14, 7467.

van Mantgem, P.J., Stephenson, N.L., 2007. Apparent climatically induced increase of tree mortality rates in a temperate forest. Ecol. Lett. 10, 909–916.

McIntyre, P.J., Thorne, J.H., Dolanc, C.R., Flint, A.L., Flint, L.E., Kelly, M., Ackerly, D.D., 2015. Twentieth-century shifts in forest structure in California: denser forests, smaller trees, and increased dominance of oaks. Proc. Natl. Acad. Sci. 112, 1458–1463.

Meyer, M.D., A. Wuenschel, and M. Slaton. 2019. Indiana Summit Research Natural Area Post- Fire Ecological Assessment.

Morrison, M.L., Raphael, M.G., 1993. Modeling the Dynamics of Snags. Ecol. Appl. 3, 322–330.

Ng, J., North, M.P., Arditti, A.J., Cooper, M.R., Lutz, J.A., 2020. Topographic variation in tree group and gap structure in Sierra Nevada mixed-conifer forests with active fire regimes. For. Ecol. Manag. 472, 118220.

North, M.P., Van de Water, K.M., Stephens, S.L., Collins, B.M., 2009. Climate, Rain Shadow, and Human-Use Influences on Fire Regimes in the Eastern Sierra Nevada, California, USA. Fire Ecol. 5, 20–34.
North, M.P., Collins, B.M., Stephens, S.L., 2012. Using fire to increase the scale, benefits and future maintenance of fuels treatments. J. For. 110 (7), 392–401, 492-401.
Oksanen, J., G.L. Simpson, F.G. Blanchet, R. Kindt, P. Legendre, P.R. Minchin, R. B. O'Hara, P. Solymos, M.H.H. Stevens, E. Szoecs, H. Wagner, M. Barbour, M. Bedward, B. Bolker, D. Borcard, G. Carvalho, M. Chirico, M.D. Caceres, S. Durand, H.B.A. Evangelista, R. FitzJohn, M. Friendly, B. Furneaux, G. Hannigan, M.O. Hill, L. Lahti, D. McGlinn, M.-H. Ouellette, E.R. Cunha, T. Smith, A. Stier, C.J.F.T. Braak, and J. Weedon. 2024, May 21. vegan: Community Ecology Package.
Pebesma, E., R. Bivand, E. Racine, M. Sumner, I. Cook, T. Keitt, R. Lovelace, H. Wickham, J. Ooms, K. Müller, T.L. Pedersen, D. Baston, and D. Dunnington. 2024, March 24. sf: Simple Features for R.
Petrie, M.D., Hubbard, R.M., Bradford, J.B., Kolb, T.E., Noel, A., Schlaepfer, D.R., Bowen, M.A., Fuller, L.R., Moser, W.K., 2023. Widespread regeneration failure in ponderosa pine forests of the southwestern United States. For. Ecol. Manag. 545, 121208.
Plotkin, J.B., Muller-Landau, H.C., 2002. Sampling the species composition of a landscape. Ecology 83, 3344–3356.
Pusina, T., Lackovic, P., Moghaddas, J., 2023. Fire and Fuels Specialist Report. Eastern Sierra Climate and Communities Resilience Project. Page 51. Whitebark Institute.
Safford, H.D., and J.T. Stevens. 2017. Natural range of variation for yellow pine and mixed-conifer forests in the Sierra Nevada, southern Cascades, and Modoc and Inyo National Forests, California, USA. Page PSW-GTR-256. U.S. Department of Agriculture, Forest Service, Pacific Southwest Research Station, Albany, CA.
Sánchez Meador, A. 2024, February 8. Patch Delineation Package.
Reineke, L.H., 1933. Perfecting a stand-density index for even-aged forest. J. Agric. Researc 46, 627–638.
Sakamoto, Y., Ishiguro, M., Kitagawa, G., 1986. Akaike Information Criterion Statistics. D. Reidel Publishing Company.
Sánchez Meador, A.J., Parysow, P.F., Moore, M.M., 2011. A new method for delineating tree patches and assessing spatial reference conditions of ponderosa pine forests in Northern Arizona. Restor. Ecol. 19, 490–499.
Slaton, M.R., Holmquist, J.G., Meyer, M., Andrews, R., Beidl, J., 2019. Traditional ecological knowledge used in forest restoration benefits natural and cultural resources: the intersection between pandora moths, jeffrey pine, people, and fire. Nat. Areas J. 39, 461–471.
Speer, J., 2010. Fundamentals of Tree Ring Research. University of Arizona Press.
Stephens, S.L., Moghaddas, J.J., 2005. Fuel treatment effects on snags and coarse woody debris in a Sierra Nevada mixed conifer forest. For. Ecol. Manag. 214, 53–64. https://doi.org/10.1016/j.foreco.2005.03.055.
Stephens, S.L., Foster, D.E., Battles, J.J., Bernal, A.A., Collins, B.M., Hedges, R., Moghaddas, J.J., Roughton, A.T., York, R.A., 2024. Forest restoration and fuels reduction work: Different pathways for achieving success in the Sierra Nevada. Ecol. Appl. 34, e2932.
Stevens, J.T., 2017. Scale-dependent effects of post-fire canopy cover on snowpack depth in montane coniferous forests. Ecol. Appl. 27, 1888–1900.
Stokes, M.A., 1968. An introduction to tree-ring dating. University of Chicago Press, Chicago.
Swetnam, T.W., Allen, C.D., Betancourt, J.L., 1999. APPLIED HISTORICAL ECOLOGY: USING THE PAST TO MANAGE FOR THE FUTURE. Ecol. Appl. 9, 18.
Taylor, A.H., Halpern, C.B., 1991. The structure and dynamics of *Abies magnifica* forests in the southern Cascade Range, USA. J. Veg. Sci. 2, 189–200.
Taylor, A.H., Trouet, V., Skinner, C.N., Stephens, S., 2016. Socioecological transitions trigger fire regime shifts and modulate fire–climate interactions in the Sierra Nevada, USA, 1600–2015 CE. Proc. Natl. Acad. Sci. 113, 13684–13689.
Taylor, D.W. 1982. Ecological Survey of the vegetation of lndiana Summit Research Natural Area, Inyo National Forest, California.
Tomiolo, S., Harsch, M.A., Duncan, R.P., Hulme, P.E., Tomiolo, S., Harsch, M.A., Duncan, R.P., Hulme, P.E., 2016. Influence of climate and regeneration microsites on Pinus contorta invasion into an alpine ecosystem in New Zealand. AIMS Environ. Sci. 3, 525–540.
Urgenson, L.S., Nelson, C.R., Haugo, R.D., Halpern, C.B., Bakker, J.D., Ryan, C.M., Waltz, A.E.M., Belote, R.T., Alvarado, E., 2018. Social perspectives on the use of reference conditions in restoration of fire-adapted forest landscapes. Restor. Ecol. 26, 987–996.
USGCRP, 2018. Fourth National Climate Assessment. U.S. Global Change Research Program, Washington, DC, pp. 1–470.
Van de Water, K.M., Safford, H.D., 2011. A summary of fire frequency estimates for california vegetation before euro-American Settlement. Fire Ecol. 7, 26–58.
Wagtendonk, J.W., van, N.G., Sugihara, S.L., Stephens, A.E., Thode, 2018. In: Shaffer, K. E., Fites-Kaufman, J.A. (Eds.), Fire in California's Ecosystems. Second edition.